

Predicting machine's performance data using the stacked long short-term memory (LSTM) neural networks

Jianrong Dai (✉ Dai_jianrong@cicams.ac.cn)

Research

Keywords: long short-term memory networks (LSTM), daily QA, machine performance check (MPC), predictive time series, radiotherapy

Posted Date: October 11th, 2021

DOI: <https://doi.org/10.21203/rs.3.rs-961567/v1>

License: © ⓘ This work is licensed under a Creative Commons Attribution 4.0 International License.

[Read Full License](#)

1 Predicting machine's performance data using the stacked long short-term
2 memory (LSTM) neural networks

3 Min Ma¹, Jianrong Dai^{1#}

4 ¹ Department of Radiation Oncology, National Cancer Center/National Clinical
5 Research Center for Cancer/Cancer Hospital, Chinese Academy of Medical Sciences
6 and Peking Union Medical College, Beijing, 100021, China

7

8 **#Corresponding author**

9

10 Jianrong Dai, PhD
11 Department of Radiation Oncology
12 National Cancer Center/National Clinical Research Center for Cancer/Cancer
13 Hospital, Chinese Academy of Medical Sciences and Peking Union Medical College
14 Beijing 100021, China
15 Tel: 86-10-8778-8893
16 Email: dai_jianrong@cicams.ac.cn

17 **Abstract**

18 **Purpose:** Machine Performance Check (MPC) is a daily quality assurance (QA) tool
19 for Varian machines. The daily QA data based on MPC tests show machine
20 performance patterns and potentially provide warning messages for preventive actions.
21 This study developed a neural network model that could predict the trend of data
22 variations quantitatively.

23 **Methods and materials:** MPC data used were collected daily for 3 years. The
24 stacked long short-term memory (LSTM) model was used to develop the neural work
25 model. To compare the stacked LSTM, the autoregressive integrated moving average
26 model (ARIMA) was developed on the same data set. Cubic interpolation was used to
27 double the amount of data to enhance prediction accuracy. After then, the data were
28 divided into 3 groups: 70% for training, 15% for validation, and 15% for testing. The
29 training set and the validation set were used to train the stacked LSTM with different
30 hyperparameters to find the optimal hyperparameter. Furthermore, a greedy
31 coordinate descent method was employed to combine different hyperparameter sets.
32 The testing set was used to assess the performance of the model with the optimal
33 hyperparameter combination. The accuracy of the model was quantified by the mean
34 absolute error (MAE), root-mean-square error (RMSE), and coefficient of
35 determination (R^2).

36 **Results:** A total of 867 data were collected to predict the data for the next 5 days. The
37 mean MAE, RMSE, and R^2 with all MPC tests was 0.013, 0.020, and 0.853 in
38 LSTM, while 0.021, 0.030, and 0.618 in ARIMA, respectively. The results show that
39 the LSTM outperforms the ARIMA.

40 **Conclusions:** In this study, the stacked LSTM model can accurately predict the daily
41 QA data based on MPC tests. Predicting future performance data based on MPC tests
42 will foresee possible machine failure, allowing early machine maintenance and
43 reducing unscheduled machine downtime.

44 **Keywords:** long short-term memory networks (LSTM), daily QA, machine
45 performance check (MPC), predictive time series, radiotherapy
46

47 **1. Introduction**

48 Linear accelerators (linacs) undergo daily quality assurance (QA) testing to ensure
49 that radiation treatments are delivered safely and accurately, and that they meet the
50 quality and safety criteria of AAPM TG 142 [1]. Daily QA testing are normally
51 performed by the radiotherapist using a conventional QA instrument/ phantom.

52 The Machine Performance Check (MPC) is used for daily QA on the Varian linacs
53 (Varian Medical Systems, Inc., Palo Alto, CA). MPC is a fully integrated KV and MV
54 image-based tool to assess the performance of linac [2]. There are 2 types of MPC
55 tests: beam constancy checks and geometric testing. First, beam constancy checks
56 assess the output, beam center, and uniformity constancy against a user-defined
57 baseline. Second, geometric tests evaluate the radiation isocenter size, the coincidence
58 of MV and KV isocenters, collimator and gantry angle accuracy, jaw and multi-leaf
59 collimator leaf accuracy positions, and couch pitch and roll accuracy. All tests are
60 highly automated, and the user only should set up the IsoCal phantom and bracket on
61 the treatment couch, then beam on for the predetermined energy. MPC application has
62 been evaluated as a linac daily QA tool by some investigators [2-6].

63 The daily MPC result is used to track on the linac's long-term stability when
64 processing large quantities of data. With those data, medical physicists could calibrate
65 data baseline and monitor the linac's state to predict variation cycles and take
66 preventive actions. To understand the underlying structure and functions that produce
67 the observed tests in MPC, an appropriate modeling tool is needed to extract and
68 analyze the longitudinal daily MPC data and predict future trends.

69 These sequential sets of daily MPC data measured over successive days can be
70 considered time series. Therefore, in the context of time-series predictive modeling,
71 the question of predicting the future trend and variations has been raised [7].
72 Traditionally, statistical modeling techniques like to autoregressive integrated moving
73 average model (ARIMA) [8] and their variations (AR, MA, ARMA) [9-11], which
74 only capture the linear elements of the time series and may not be sufficient for the
75 daily QA data. Non-linear time series are best analyzed using recurrent neural
76 network (RNN). However, RNN is difficult to deal with long time series [12].
77 Therefore, the long short-term memory (LSTM) network is proposed to tackle the
78 forgetting problem [13], a type of RNN. LSTM has shown good performance in
79 various fields (finance, public transportation, astronomy, environmental science, and
80 medicine) [12]. In the previous studies of the predictive model development about
81 daily QA in linac, Li and chan (2017) [7] used artificial neural networks (ANN), and

82 ARMA on 5-year daily beam QA data, which showed ANN had better prediction
83 performance than ARMA. Puyati et al. (2020) [14] used statistical process control and
84 ARIMA to forecast QA. However, there is poor performance to predict QA data in
85 linac or trends and exist time lags in the predictive model.

86 A generalized LSTM model was developed to predict daily QA data/trend based on
87 MPC tests in this study. Additionally, this study emphasized discovering the common
88 behaviors of the linac performance so that physicists could be more confident in
89 predicting the machine's future behavior and taking action in a planned way before
90 the tolerance level is reached. Finally, to compare and provide context for our results,
91 we also developed a prediction model with ARIMA on the same data set.

92

93 **2. Methods and material**

94 **2.1. Data acquisition**

95 MPC is designed to examine and evaluate the machine's performance about 5 min
96 before starting the routine treatment. 24 MPC tests were run, including isocenter,
97 collimation, gantry, and couch tests. Daily MPC data were collected at our institution
98 using Varian Edge (Varian Medical Systems, Palo Alto, CA) for more than 3 years,
99 from August 2017 to October 2020. We presented results for beam data predictive
100 modeling in this study.

101

102 **2.2. Data pre-processing**

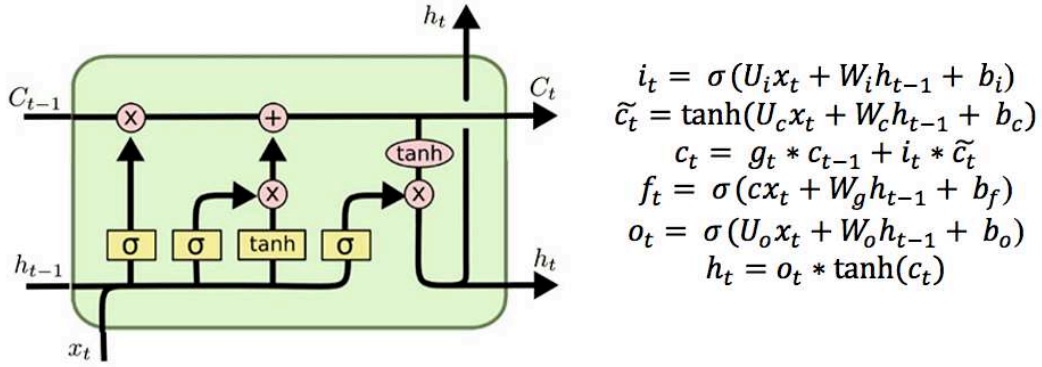
103 Pre-processing data is a significant step before building a model. In this study,
104 performing data pre-processing included cleaning, interpolation, normalization, and
105 data split. The duplicate data was deleted at the starting point. Cubic interpolation was
106 used to double the amount of data to improve the prediction accuracy. The data was
107 normalized for the model, ranging from -1 to 1 . The data was divided into 3 sets: 70%
108 for training, 15% for validation, and 15% for testing. The training set and the
109 validation set was used to train the model with different hyperparameter combinations
110 (see section 2.3.2). The testing set was used to assess the performance of the model
111 with the optimal hyperparameter combination.

112

113 **2.3. Building LSTM network**

114 **2.3.1 LSTM network**

115 LSTM is very powerful in solving sequence prediction problems because it can
116 store previous information [15], which is essential to predict the future data/trend of
117 MPC daily QA data. Through the standard recurrent layer, self-loops, and the internal
118 unique gate structure, the LSTM network effectively improves the forgetting and
119 gradient vanishing problem existing in the traditional RNN [13]. Besides, LSTM can
120 learn to make a one-shot multi-step prediction useful for predicting the time series.
121 An LSTM neural network unit combines 4 gates: an input gate, a cell state, a
122 forgotten gate, and an output gate (Fig. 1) [16].



124 Figure 1. The structure of LSTM as described by Varsamopoulos (2018) [18]. input
 125 gate (i_t), input module gate (\tilde{c}_t), forget gate (f_t), and output gate (o_t). b is bias vectors,
 126 c_t is cell state, h_t is the hidden state, and σ is the sigmoid activation function. All
 127 these controllers determine how much information to receive from the last loop, and
 128 how much to pass to the new state.

129
 130 The forget gate is used to determine which messages pass through the cell, then
 131 enter the input gate, which decides how many new messages to add to the cell state,
 132 and finally decide the output message through the output gate [17].

133 The original LSTM model is comprised of a single hidden LSTM layer followed by
 134 a standard feedforward output layer. The stacked LSTM is an extension to this model
 135 that has multiple hidden LSTM layers where each layer contains multiple memory
 136 cells [12]. The stacked LSTM hidden layers make the model deeper, more accurately
 137 earning the description as a deep learning technique. It is the depth of neural networks
 138 that are attributed to the approach's success on various challenging prediction
 139 problems [19]. The stacked LSTM is now a stable technique for challenging sequence
 140 prediction problems [20]. An LSTM model with many LSTM layers is a stacked
 141 LSTM architecture (Fig. 2) [21]. An LSTM layer above provides a sequence output
 142 rather than a single value output to the LSTM layer below. Specifically, one output
 143 per input time step is one output time step for all input time steps. Therefore, in this
 144 study, the stacked LSTM was selected.

145



147 Figure 2. The stacked LSTM architecture.

148

149 For the ARIMA, there are 3 critical parameters in ARIMA: p (the past value used
 150 to predict the next value), q (past prediction error used to predict future values), and d
 151 (order of differencing) [22, 23]. ARIMA parameter optimization requires much time.
 152 Therefore, in this study, ARIMA selects the combination (5, 1, 0).

153

154 2.3.2. Model training

155 The experiment's LSTM model is built on the Keras API package (TensorFlow2.0)
156 in Python 3.6 settings (Python Software Foundation, Wilmington, DE). In this study,
157 networks with two LSTM layers were investigated. The loss value was evaluated by
158 the root-mean-square error (RMSE). The activation functions used the rectified linear
159 units (Relu) function. A greedy coordinate descent method [24] was employed to find
160 the optimal hyperparameter of the model.

161 The length of time lags, the optimizers, the learning rates, the number of epochs,
162 the number of hidden units, and the batch sizes were among the tuning parameters.
163 First, we sought to find the optimal length of time lags when the optimizer was Adam,
164 the learning rate was 0.01, the number of epochs was 150, the number of hidden units
165 was 50, and the batch sizes were 32. Subsequently, we determined the type of
166 optimizer with the optimal length of time lags. Next, the appropriate learning rate was
167 determined by comparing results from various learning rates. Then, we sought to find
168 the optimal number of epochs and hidden units in turn. Lastly, to determine the
169 optimal batch size, a similar comparison was performed. The batch size was adjusted
170 to avoid errors from memory shortage. By testing the parameter values of different
171 combinations, and the model suitable for the data was finally found. The tuning
172 hyperparameters were presented in section 2.3.3.

173

174 2.3.3 Hyperparameters optimization

175 Hyperparameters selection and optimization play an important role in obtaining
176 superior accuracy with the LSTM network [25]. The validation set's mean absolute
177 error (MAE) was used to evaluate the model's performance for each parameter
178 combination. The following hyperparameters were investigated for the stacked LSTM
179 network:

180 (1) Length of time lags – A time lag refers to a sequence of daily MPC QA data
181 acting as the stacked LSTM model's input. The length of time lag represents the
182 number of intakes to make a prediction, and different lengths of time lag may cause
183 different prediction results.

184 (2) Optimizer – The optimizer is in charge of minimizing the stacked LSTM model's
185 objective function.

186 (3) Learning rate – The optimizer's performance is affected by the learning rate. The
187 learning rate determines how much the weight is updated at the end of each batch.

188 (4) Number of epochs – The number of epochs specifies how many times the stacked
189 LSTM model traverses the whole training dataset. Each sample in the training dataset
190 has the opportunity to update the internal model parameters once every epoch.

191 (5) Number of hidden units per layer – The number of neurons in a layer controls the
192 representational capacity of the network. The same value for each LSTM layer was
193 assigned.

194 (6) Batch size – In iterative gradient descent, the batch size refers to the number of
 195 patterns that are given to the network before the weights are updated. It is also a
 196 training optimization for the network, determining how many patterns to read and
 197 keep in memory.

198

199 **2.4. Evaluation of predictive accuracy**

200 To evaluate the error between the predicted and observed values in the testing set,
 201 the RMSE, MAE, and coefficient of determination (R^2) was selected.

202

203 **2.5. The trend lines**

204 The trend lines were used to analyze the trend of linac operating status and thereby
 205 help medical physicists decide whether to take preventive actions. The stacked LSTM
 206 model was applied to predict the next-5-day daily MPC results in this study. The trend
 207 lines were plotted by the polynomial fit from five-step-head predictive values.

208

209 **3. Results**

210 **3.1. Hyperparameter tuning in LSTM**

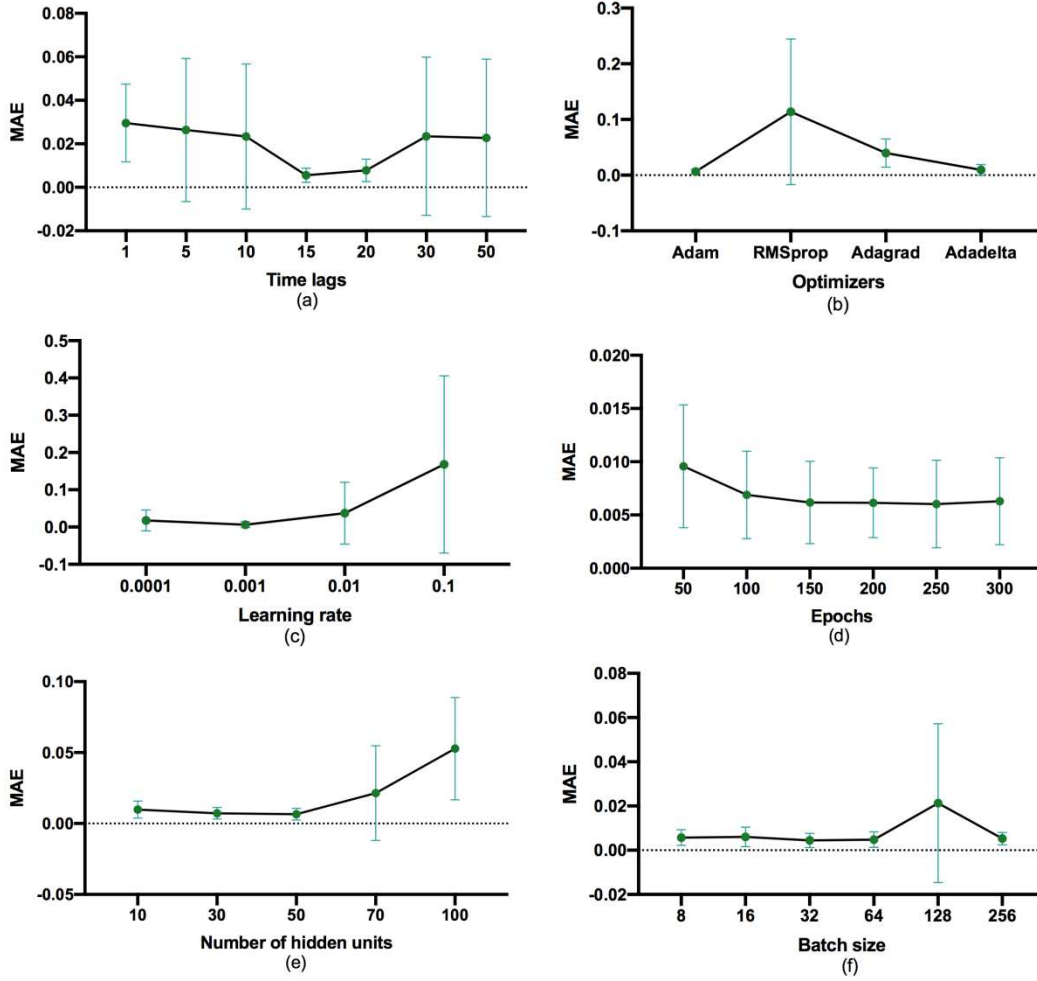
211 Figure 3 shows the MAE (in a relative unit) as a function of time lags, optimizers,
 212 learning rates, epochs, hidden units, and batch sizes. The optimal hyperparameter
 213 value is summarized in Table 1. Among them, the learning rate had the greatest
 214 impact on the model. The best performance was set to 0.001 of the learning rates, and
 215 the worst was set to 0.1, causing up to 0.039 difference in relative MAE. Furthermore,
 216 the type of optimizer had the second greatest impact on the model. In comparison, the
 217 length of time lags and the number of hidden units demonstrated only a modest
 218 impact on the model's predictive performance. Finally, the number of epochs and the
 219 batch size showed little impact on the predictive accuracy.

220

221

222 Table 1. The summary of LSTM hyperparameters investigated in this study, and the
 223 recommended configurations, and the impact level of each parameter.

Hyperparameters	Range	Recommended configuration	Impact
Length of time lags	{1, 5, 10, 15, 20, 30, 50}	15	Middle
Optimizer	{Adam, RMSprop, Adagrad, Adadelta}	Adam	High
Learning rate	{0.0001, 0.001, 0.01, 0.1}	0.001	High
Number of epochs	{50, 100, 150, 200, 250, 300}	300	Low
Number of hidden units per layer	{10, 30, 50, 70, 100}	50	Middle
Batch size	{8, 16, 32, 64, 128, 256}	32	Low



225
 226 Figure 3. The MAE of predicted data (mean value in green, 95%CI in blue) with
 227 different values of different (a) the length of time lags, (b) the optimizers, (c) the
 228 learning rates, (d) the number of epochs, (e) the number of hidden units, and (f) the
 229 batch sizes. MAE is the mean absolute error.

230

231 3.2. Predictive performance evaluation

232 A total of 867 data is collected to predict the data for the next 5 days. Table 2
 233 shows the performance of the stacked LSTM model in predicting daily MPC tests
 234 using the optimal hyperparameter and ARIMA. The mean MAE, RMSE, and R^2
 235 with all MPC tests was 0.013, 0.020, and 0.853 in LSTM, while 0.021, 0.030, and
 236 0.618 in ARIMA, respectively. LSTM performs better than ARIMA in 23 MPC items
 237 with the smaller MAE value, smaller RMSE value, and higher R^2 , except for gantry
 238 relative (LSTM: MAE = 0.006, RMSE = 0.007 and $R^2 = 0.095$; ARIMA: MAE =
 239 0.004, RMSE = 0.006 and $R^2 = 0.383$). The best predictive performance of LSTM
 240 was couch rotation (MAE = 0.001, RMSE = 0.004 and $R^2 = 0.975$), but the worst
 241 was gantry relative (MAE = 0.006, RMSE = 0.007 and $R^2 = 0.095$). Additionally,
 242 Figure 4 shows the comparison of model performance in terms of the coefficient of

243 determination (R^2). The R^2 value of LSTM is higher point than ARIMA in Figure 4,
 244 except for the R^2 value of gantry relative. In general, LSTM outperforms the
 245 ARIMA.

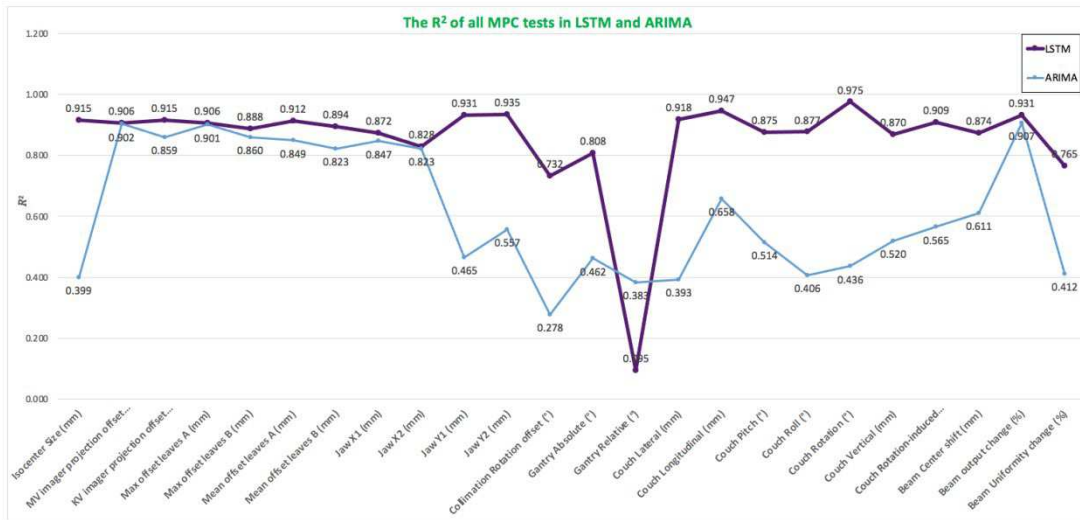
246 Figure 5 depicts 3 representative cases (beam center shift, beam output change, and
 247 beam uniformity change) of the observed versus the predicted curves using the
 248 stacked LSTM model with the optimal hyperparameter combination in testing data.
 249

250 Table 2. Results of the stacked LSTM and ARIMA model evaluation.

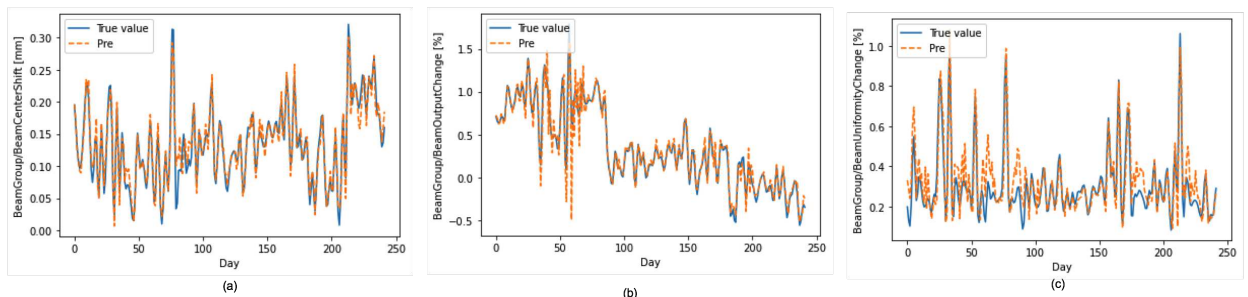
MPC test		MAE		RMSE		R2	
Categories	Test	LSTM	ARIMA	LSTM	ARIMA	LSTM	ARIMA
Isocenter	Size (mm)	0.002	0.006	0.003	0.008	0.915	0.399
	MV imager projection offset (mm)	0.010	0.013	0.020	0.020	0.906	0.902
	KV imager projection offset (mm)	0.013	0.015	0.018	0.024	0.915	0.859
Collimation	Max offset leaves A (mm)	0.010	0.009	0.012	0.013	0.906	0.901
	Max offset leaves B (mm)	0.008	0.008	0.010	0.012	0.888	0.860
	Mean offset leaves A (mm)	0.007	0.009	0.010	0.013	0.912	0.849
	Mean offset leaves B (mm)	0.006	0.008	0.008	0.011	0.894	0.823
	Jaw X1 (mm)	0.012	0.013	0.018	0.019	0.872	0.847
	Jaw X2 (mm)	0.011	0.013	0.019	0.019	0.828	0.823
	Jaw Y1 (mm)	0.017	0.044	0.022	0.062	0.931	0.465
	Jaw Y2 (mm)	0.017	0.043	0.022	0.057	0.935	0.557
Gantry	Rotation offset (°)	0.030	0.047	0.039	0.064	0.732	0.278
	Absolute (°)	0.003	0.006	0.005	0.008	0.808	0.462
Couch	Relative (°)	0.006	0.004	0.007	0.006	0.095	0.383
	Lateral (mm)	0.005	0.012	0.006	0.016	0.918	0.393
Couch	Longitudinal (mm)	0.004	0.010	0.006	0.014	0.947	0.658
	Pitch (°)	0.001	0.002	0.002	0.003	0.875	0.514
	Roll (°)	0.002	0.004	0.002	0.005	0.877	0.406
	Rotation (°)	0.001	0.002	0.001	0.004	0.975	0.436
	Vertical (mm)	0.008	0.016	0.011	0.021	0.870	0.520
	Rotation-induced couch shift (mm)	0.008	0.017	0.011	0.024	0.909	0.565
	Beam	Center shift (mm)	0.014	0.027	0.021	0.037	0.874
Beam output change (%)		0.069	0.098	0.120	0.139	0.931	0.907
Uniformity change (%)		0.054	0.082	0.078	0.129	0.765	0.412
Mean		0.013	0.021	0.020	0.030	0.853	0.618

251

252 Abbreviations: MAE = mean absolute error, RMSE = root - mean-square error, $R^2 =$
 253 coefficient of determination.
 254



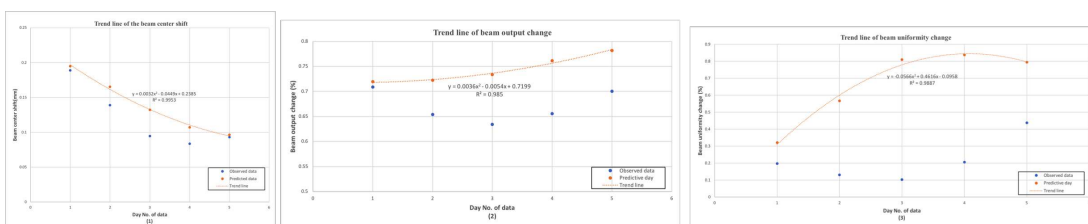
256 Figure 4. Comparison graph of model performance in the coefficient of determination
 257 (R^2). The purple line means LSTM, and the blue line means ARIMA.



259 Figure 5. Comparison of predicted and observed beam QA results, including (a) beam
 260 center shift, (b) beam output change, and (c) beam uniformity change using the
 261 stacked LSTM model with the optimal hyperparameters in testing data.
 262

263 3.3. The trend lines

264 The weekly trend line for the beam is shown in Figure 6. All predictive values were
 265 within the tolerance. The trend was that the beam center shift drop but remains at
 266 normal-stage levels. The trend of the beam output change and beam uniformity
 267 change rose, located in the normal range. This provides the opportunity to adjust the
 268 machine.



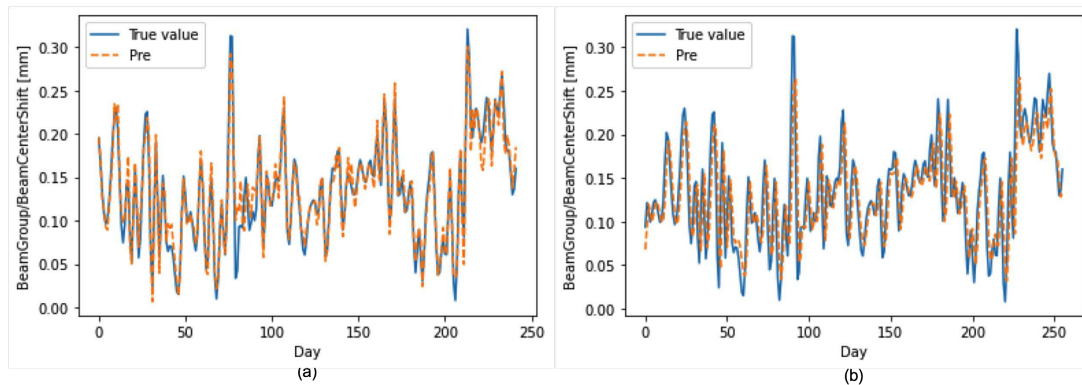
270 Figure 6. An example of the trend line to detect (a) the beam center shift, (b) beam
271 output change, and (c) beam uniformity change.

272

273 4. Discussion

274 4.1. Impact of hyperparameters

275 This study demonstrates the need to tuning the hyperparameter using a deep
276 LSTM model for daily MPC testing to obtain good predictive results. The learning
277 rate determines how fast your neural net “learns.” If the learning rate is too high, our
278 loss will start jumping all over the place and never converge [26]. If the learning rate
279 is too low, the model will take way too long to converge [26], as illustrated above.
280 The challenge of using a learning rate is that their hyperparameters must be defined in
281 advance, and they depend heavily on the type of model and problem. Adaptive
282 gradient descent algorithms (Adagrad, Adadelata, RMSprop, Adam) provide a
283 heuristic approach without requiring expensive work to manually tuning
284 hyperparameters for the learning rate [27]. According to the MAE value (Fig. 3),
285 Adam and learning rate setting to 0.001 was recommended to use in the stacked
286 LSTM model. Besides, when adjusting the different lengths of time lags, the LSTM
287 predictive effect will be delayed (Fig. 7). R^2 value of the beam center shift is 0.603
288 (the lengths of time lag = 1), while R^2 value of the beam center shift is 0.874 (the
289 lengths of time lag = 15). Lag observations for a univariate time series can be used as
290 time lags for an LSTM model, which can improve forecast performance.



292 Figure 7. The predictive performance of the beam center shift with (a) the length of
293 time lags= 15, and (b) the length of time lags= 1 in the stacked LSTM model.

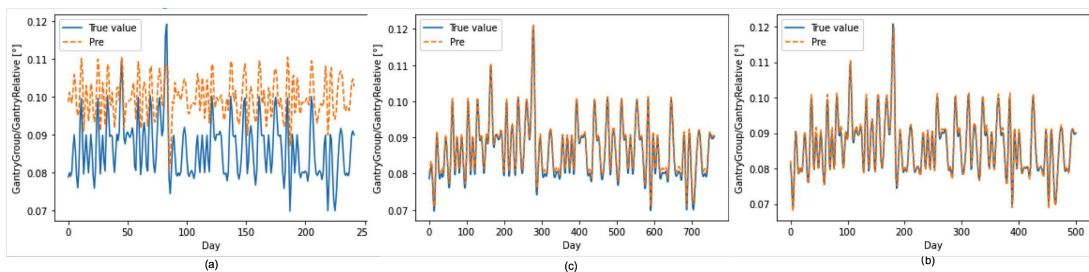
294

295 4.2. Predictive performance

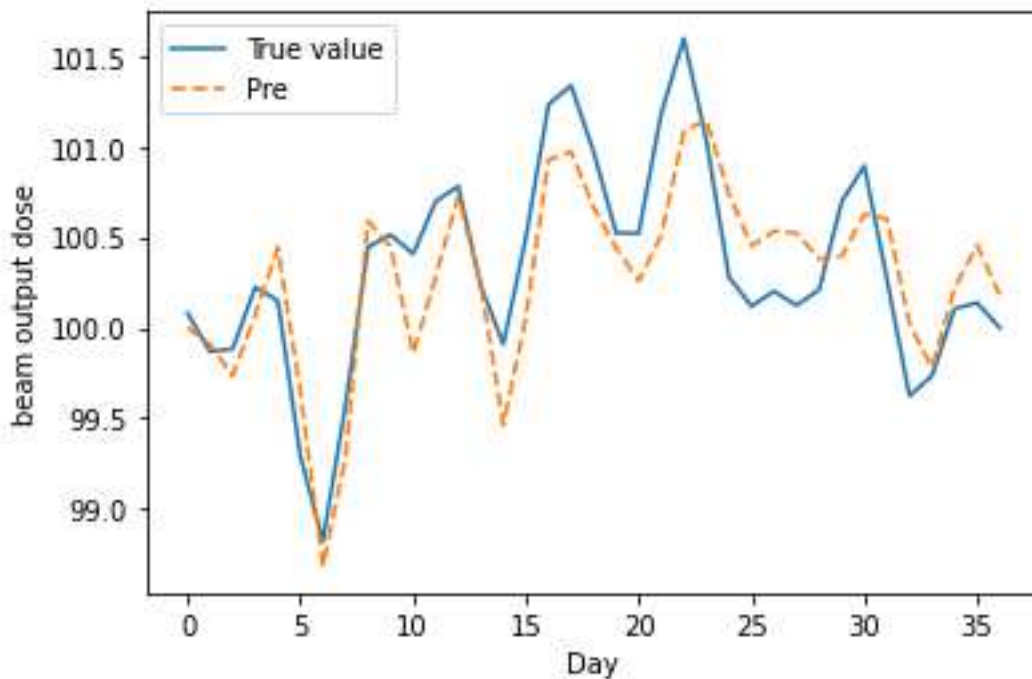
296 This is the first study to implement a stacked LSTM model for daily MPC data
297 prediction to the best of our knowledge. It is one of the first few attempts to develop
298 and evaluate a single generic stacked LSTM model. The stacked LSTM model
299 allowed connections through time and provided a way to feed the hidden layers from
300 previous steps (long-term and short-term) as additional inputs to the next stage, in
301 contrast to earlier studies that only focused on studying the power of ANN [7]. The
302 stacked LSTM is effective at predicting daily MPC data. However, the generic

303 stacked LSTM is poor in predicting the data of the gantry relative with 2 times cubic
 304 interpolation. In Figure 8(a), the predictive range is significantly shifted up and
 305 slightly delayed. According to Wang et al. (2019) study [28], we guess that LSTM
 306 predictive performance is related to the signal frequency. Interpolation reduces
 307 high-frequency signals and can greatly improve the predictive ability of the stacked
 308 LSTM model. Therefore, we try 4 times cubic interpolation and 6 times cubic
 309 interpolation in the stacked LSTM model, which significantly improves the accuracy
 310 performance (Fig. 8(b) and (c)). The predictive performance of the gantry relative
 311 with 6 times cubic interpolation is great ($R^2 = 0.978$) in the stacked LSTM model.

312 To illustrate the robustness of the model, we apply LSTM model to the QA data of
 313 output dose weekly on the Elekta's linac without changing any hyperparameters
 314 chosen for this study. The MAE, RMSE and R^2 is 0.229, 0.283, and 0.750,
 315 respectively (Fig. 9). For a clinical routine, it is unnecessary to retrain the neural
 316 network each day with the daily acquired MPC data.



318 Figure 8. The predictive performance of the gantry relative to (a) 2 times cubic
 319 interpolation, (b) 4 times cubic interpolation, and (c) 6 times cubic interpolation in the
 320 stacked LSTM model.



324

325 **4.3. The trend lines**

326 For all daily MPC tests, the predicted data locates within the clinical tolerances
 327 (AAPM TG-142) [1], providing a window of opportunity to prevent the performance
 328 issue in advance. However, in the actual situation, besides keeping parameters within
 329 the tolerance, a clinical physicist should monitor trends in the machine performance
 330 [29] and to know when the linac needs to be maintained, thereby reducing the chance
 331 of linac downtime. Here, a five-step-ahead prediction is appropriate to provide trends
 332 in linac status.

333

334 **4.4. Limitations and future work**

335 However, there exist some limitations in this study. Considering the
 336 time-consuming problem, tuning hyperparameters does not choose between the grid
 337 search, the random search, and random search. Furthermore, some hyperparameters
 338 correlate with each other and can result in different performances when optimized
 339 simultaneously rather than tuning [30]. Due to prediction models being based on large
 340 learning-phase datasets, the predictive models are not designed to detect large sudden
 341 one-off jumps in data such as might be expected with a linac component failure. Linac
 342 interlocks are still required to mitigate treatment delivery errors from such events and
 343 routine retrospective QA. Predictive QA is more suited to detecting and predicting
 344 gradual drifts and failures that repeat at regular intervals.

345 The present study results suggest that the approach of predictive QA based on MPC
346 tests is feasible, but additional data on more linacs are required. Therefore, such a
347 study is proposed as future work.

348

349 **5. Conclusions**

350 This study developed and evaluated a generalized stacked LSTM model for daily
351 MPC prediction. This model has a better performance than the ARIMA model and
352 can reduce the unscheduled linac downtime and allow linac performance parameters
353 to be controlled within tolerances in the clinic.

354

355 **CONFLICT OF INTEREST**

356 The authors have no conflicts to disclose.

357

358

359 **References**

- 360 [1] Klein EE, Hanley J, Bayouth J, Yin FF, Simon W, Dresser S, et al. Task Group 142 report:
361 Quality assurance of medical accelerators a. Medical physics. 2009;36:4197-212.
- 362 [2] Clivio A, Vanetti E, Rose S, Nicolini G, Belosi MF, Cozzi L, et al. Evaluation of the Machine
363 Performance Check application for TrueBeam Linac. Radiat Oncol. 2015;10:97.
- 364 [3] Barnes MP, Pomare D, Menk FW, Moraro B, Greer PB. Evaluation of the truebeam
365 machine performance check (MPC): OBI X-ray tube alignment procedure. J Appl Clin Med
366 Phys. 2018;19:68-78.
- 367 [4] Barnes MP, Greer PB. Evaluation of the TrueBeam machine performance check (MPC)
368 beam constancy checks for flattened and flattening filter-free (FFF) photon beams. J Appl
369 Clin Med Phys. 2017;18:139-50.
- 370 [5] Barnes MP, Greer PB. Evaluation of the truebeam machine performance check (MPC):
371 mechanical and collimation checks. J Appl Clin Med Phys. 2017;18:56-66.
- 372 [6] Barnes MP, Greer PB. Evaluation of the truebeam machine performance check (MPC)
373 geometric checks for daily IGRT geometric accuracy quality assurance. J Appl Clin Med Phys.
374 2017;18:200-6.
- 375 [7] Li Q, Chan MF. Predictive time-series modeling using artificial neural networks for Linac
376 beam symmetry: an empirical study. Annals of the New York Academy of Sciences.
377 2017;1387:84.
- 378 [8] Siami-Namini S, Tavakoli N, Siami Namin A. A Comparison of ARIMA and LSTM in
379 Forecasting Time Series. 2018 17th IEEE International Conference on Machine Learning
380 and Applications (ICMLA)2018. p. 1394-401.
- 381 [9] Tu Y-H, Peng C-C. An ARMA-Based Digital Twin for MEMS Gyroscope Drift Dynamics
382 Modeling and Real-Time Compensation. Ieee Sensors Journal. 2021;21:2712-24.
- 383 [10] Lee K, Lee C-H, Kwak M-S, Jang EJ. Analysis of multivariate longitudinal data using
384 ARMA Cholesky and hypersphere decompositions. Computational Statistics & Data Analysis.
385 2021;156.
- 386 [11] Chakraborty D, Sanyal SK. Time-series data optimized AR/ARMA model for frugal

387 spectrum estimation in Cognitive Radio. *Physical Communication*. 2021;44.

388 [12] Yu Y, Si X, Hu C, Zhang J. A Review of Recurrent Neural Networks: LSTM Cells and
389 Network Architectures. *Neural Comput*. 2019;31:1235-70.

390 [13] Hochreiter S, Schmidhuber J. Long short-term memory. *Neural Comput*.
391 1997;9:1735-80.

392 [14] Puyati W, Khawne A, Barnes M, Zwan B, Greer P, Fuangrod T. Predictive quality
393 assurance of a linear accelerator based on the machine performance check application
394 using statistical process control and ARIMA forecast modeling. *Journal of Applied Clinical
395 Medical Physics*. 2020;21:73-82.

396 [15] Gers FA, Schmidhuber J, Cummins F. Learning to forget: Continual prediction with
397 LSTM. *Neural Computation*. 2000;12:2451-71.

398 [16] Pascanu R, Mikolov T, Bengio Y. Understanding the exploding gradient problem. *ArXiv*.
399 2012;abs/1211.5063.

400 [17] Elman J. Finding Structure in Time. *Cogn Sci*. 1990;14:179-211.

401 [18] Varsamopoulos S, Bertels K, Almudever C. Designing neural network based decoders
402 for surface codes2018.

403 [19] Anastasi G, Bertholet J, Poulsen P, Roggen T, Garibaldi C, Tilly N, et al. Patterns of
404 practice for adaptive and real-time radiation therapy (POP-ART RT) part I: Intra-fraction
405 breathing motion management. *Radiotherapy and Oncology*. 2020;153:79-87.

406 [20] Li Y, Lin Z. Melody Classifier with Stacked-LSTM. *ArXiv*. 2020;abs/2010.08123.

407 [21] Fernandez S, Graves A, Schmidhuber J. Sequence Labelling in Structured Domains with
408 Hierarchical Recurrent Neural Networks. *IJCAI2007*.

409 [22] Zhang G. Time series forecasting using a hybrid ARIMA and neural network model.
410 *Neurocomputing*. 2003;50:159-75.

411 [23] Box G, Jenkins G. *Time series analysis, forecasting and control*. 1970.

412 [24] Dhillon I, Ravikumar P, Tewari A. Nearest Neighbor based Greedy Coordinate Descent.
413 *NIPS2011*.

414 [25] Greff K, Srivastava R, Koutník J, Steunebrink BR, Schmidhuber J. LSTM: A Search Space
415 Odyssey. *IEEE Transactions on Neural Networks and Learning Systems*. 2017;28:2222-32.

416 [26] Yu C, Qi X, Ma H, He X, Wang C, Zhao Y. LLR: Learning learning rates by LSTM for
417 training neural networks. *Neurocomputing*. 2020;394:41-50.

418 [27] Zaheer R, Shaziya H. A Study of the Optimization Algorithms in Deep Learning. 2019
419 Third International Conference on Inventive Systems and Control (ICISC). 2019:536-9.

420 [28] Wang S, Li C, Lim A. Why Are the ARIMA and SARIMA not Sufficient. *ArXiv*.
421 2019;abs/1904.07632.

422 [29] Chan MF, Li Q, Tang X, Li X, Li J, Tang G, et al. Visual Analysis of the Daily QA Results of
423 Photon and Electron Beams of a Trilogy Linac over a Five-year Period. *International journal
424 of medical physics, clinical engineering and radiation oncology*. 2015;4:290-9.

425 [30] Lin H, Shi C, Wang B, Chan MF, Tang X, Ji W. Towards real-time respiratory motion
426 prediction based on long short-term memory neural networks. *Phys Med Biol*.
427 2019;64:085010.

428